

Enhanced light extraction efficiency from AlGaInP thin-film light-emitting diodes with photonic crystals

K. Bergenek,^{1,2,a)} Ch. Wiesmann,¹ R. Wirth,¹ L. O'Faolain,² N. Linder,¹ K. Streubel,¹ and T. F. Krauss²

¹OSRAM Opto Semiconductors GmbH, Leibnizstr. 4, 93055 Regensburg, Germany

²University of St Andrews, School of Physics and Astronomy, St. Andrews, Fife KY16 9SS, United Kingdom

(Received 16 May 2008; accepted 2 July 2008; published online 29 July 2008)

We investigate the use of photonic crystals for light extraction from high-brightness thin-film AlGaInP light-emitting diodes with different etch depths, lattice constants, and two types of lattices (hexagonal and Archimedean). Both simulations and experimental results show that the extraction of high order modes with a low effective index n_{eff} is most efficient. The highest external quantum efficiency without encapsulation is 19% with an Archimedean A7 lattice with reciprocal lattice constant $G=1.5 k_0$, which is 47% better than an unstructured reference device. © 2008 American Institute of Physics. [DOI: 10.1063/1.2963030]

Total internal reflection at the semiconductor-air interface results in poor light extraction efficiency from light-emitting diodes (LEDs). Photonic crystals (PhC) have already been applied to extract the guided light.¹ Following initial concentration on infrared PhC-LEDs,^{2,3} recent developments have focussed on GaN-based LEDs.⁴⁻⁶ Furthermore, quasicrystals, such as Archimedean lattices, have also been implemented to allow for omnidirectional light extraction.³ It is still uncertain, however, whether PhC-LEDs can outperform state-of-the-art LEDs in terms of external quantum efficiency η_{QE} . Here, we investigate the use of PhCs for light extraction from high efficiency thin-film LEDs in the AlGaInP material system emitting at 650 nm and compare the experimental results with simulations.

The PhC diffracts guided modes with in-plane wave vector $k_i = |n_{\text{eff},i}|k_0$ ($1 < |n_{\text{eff},i}| < n_{\text{QW}}$) as seen in Fig. 2(a) according to Bragg's law

$$\mathbf{n}_{\text{eff},d}(k_x, k_y) = \mathbf{n}_{\text{eff},i}(k_x, k_y) + \mathbf{G}/k_0, \quad (1)$$

where n_{eff} is the effective index of the mode, G is a reciprocal lattice vector of the PhC, and k_0 is the vacuum wavenumber. Diffracted modes with $0 < |n_{\text{eff},d}| < 1$ are extracted to air with the farfield angle $\theta = \sin^{-1}(n_{\text{eff},d})$. Hence, a mismatch $\Delta = |\mathbf{n}_{\text{eff},i} - \mathbf{G}/k_0| < 1$ is allowed for first order diffraction to air but the extraction efficiency for large Δ is low as it is proportional to $\sqrt{1-\Delta^2}$.⁷ Since guided modes in AlGaInP have $n_{\text{eff}} \in [1, 3.4]$, the optimal reciprocal lattice constant must be sought in the range $1 < G/k_0 < 3.4$.

Our LEDs were grown by metal-organic vapor phase epitaxy on a GaAs substrate and processed according to the scheme described elsewhere.⁸ The vertical refractive index structure of the LED can be seen in Fig. 1. It has a combined transparent conductive oxide/Au mirror and p contact. The active region consists of five GaInP quantum wells (QWs) with $(\text{Al}_{0.5}\text{Ga}_{0.5})_{0.5}\text{In}_{0.5}\text{P}$ barriers embedded between 400 nm thick AlInP electrical confinement layers. A 3.8 μm thick $n\text{-Al}_{0.6}\text{Ga}_{0.4}\text{As}$ current spreading layer ensures sufficient current spreading onto the $250 \times 250 \mu\text{m}^2$ chip. The PhCs were defined on 400 nm thick ZEP-520A resist by e-beam lithog-

raphy and subsequently etched with chlorine-based chemically assisted ion beam etching into the $n\text{-Al}_{0.6}\text{Ga}_{0.4}\text{As}$ current spreading layer using only the ZEP resist as a mask. Two sets of samples were etched to an etch depth of 200 and 800 nm, respectively. We fabricated hexagonal lattices and Archimedean A7 lattices with reciprocal lattice constant G between $1.5 k_0$ and $3.4 k_0$, corresponding to lattice constants between 490 and 224 nm, respectively [Figs. 2(b) and 2(c)]. The PhC-LEDs and unpatterned reference LEDs were mounted on TO18 headers for characterization. The total flux from the fabricated LEDs was measured in an integrating sphere. The PhC enhancement at 10 mA drive current was given by dividing the PhC-LED intensity with an unpatterned reference LED intensity and is plotted in Fig. 2(d).

The experimental extraction efficiency dependence on G can be compared with a model based on coupled mode theory, where we treat the PhC as a perturbation of the unpatterned LED. Hence, we assume that the internal emission pattern is similar to the emission pattern in an unpatterned LED, where the PhC region has an effective refractive index n_{PhC} . The diffracted intensity from mode n to mode m is given by

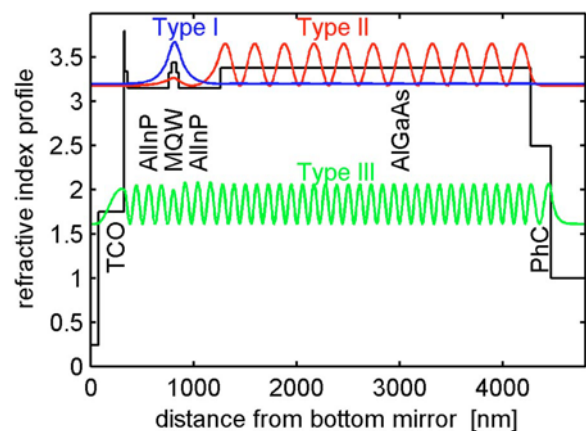


FIG. 1. (Color online) Vertical refractive index profile of the characterized LED (black thick line) and normalized guided mode intensity profiles. The high intensity type I mode is confined to the MQW region. Type II modes are evanescent in the PhC region whereas type III modes can propagate in the PhC region.

^{a)}Electronic mail: krister.bergenek@osram-os.com.

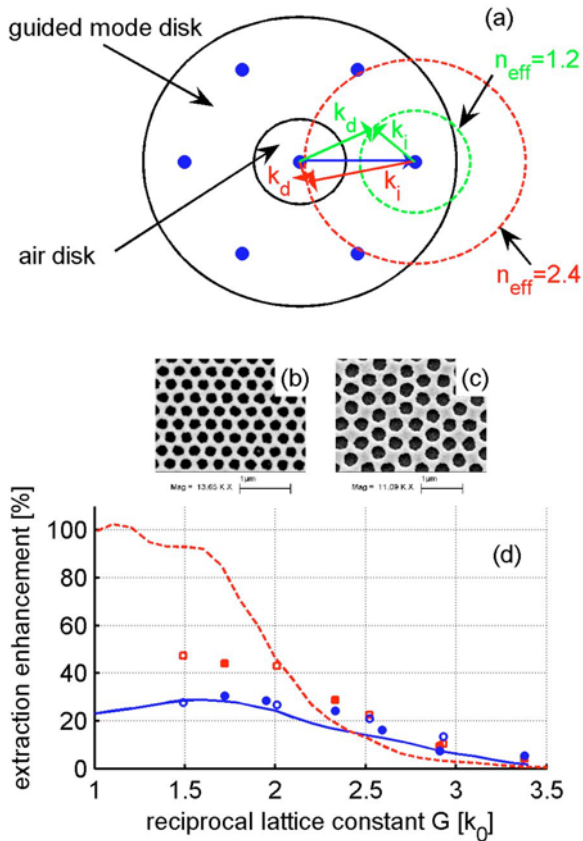


FIG. 2. (Color online) (a) Diffraction of incident in-plane k vectors k_i to k_d by the reciprocal lattice vector $G=2.5$. Both modes cannot be extracted by the same PhC. [(b) and (c)] Scanning electron microscope images of LED surfaces with a hexagonal PhC and an Archimedean A7 lattice. (d) Experimental PhC enhancements for hexagonal (filled) and A7 (open) lattices with 200 nm (circles) and 800 nm (squares) etch depth together with simulated diffraction intensity in a.u. for 200 nm (solid line) and 800 nm etch depth (dashed line).

$$I_d(n \rightarrow m) \propto I_n |\Delta \tilde{\epsilon}_{mn}|^2 |\kappa_{mn}|^2, \quad (2)$$

where I_n is the spontaneous emission into the n th mode, $|\Delta \tilde{\epsilon}_{mn}|^2$ is the Fourier amplitude of the reciprocal lattice vector G that couples mode n to m , and κ_{mn} represents the coupling strength and is calculated as

$$\kappa_{mn} = \int_{\text{PhC}} E_m^*(z) \cdot E_n(z) dz. \quad (3)$$

The diffracted intensity into air is given by summing up all diffraction events for radiating modes with $n_{\text{eff}} < 1$. The strength of this model⁷ is that the real undisturbed mode distribution is taken into account as well as all diffraction orders. Naturally, the validity of this perturbative approach decreases as the PhC etch depth increases, which is also evident from the comparison of experimental and simulated diffraction efficiencies presented in Fig. 2(d). There is good agreement for 200 nm etch depth, but less so for 800 nm. For the 200 nm curve (solid line), maximum diffraction to air is obtained for $G=1.6$. This can be understood by considering the vertical guided mode intensity profile for different types of modes in the LED (Fig. 1). A few modes with $n_{\text{eff}} > n_{\text{AlInP}}$ are resonant in the waveguide created by the high index multiple QW (MQW) region surrounded by the lower index AlInP electrical confinement layers. These so called type I modes have a very high intensity but they are hardly

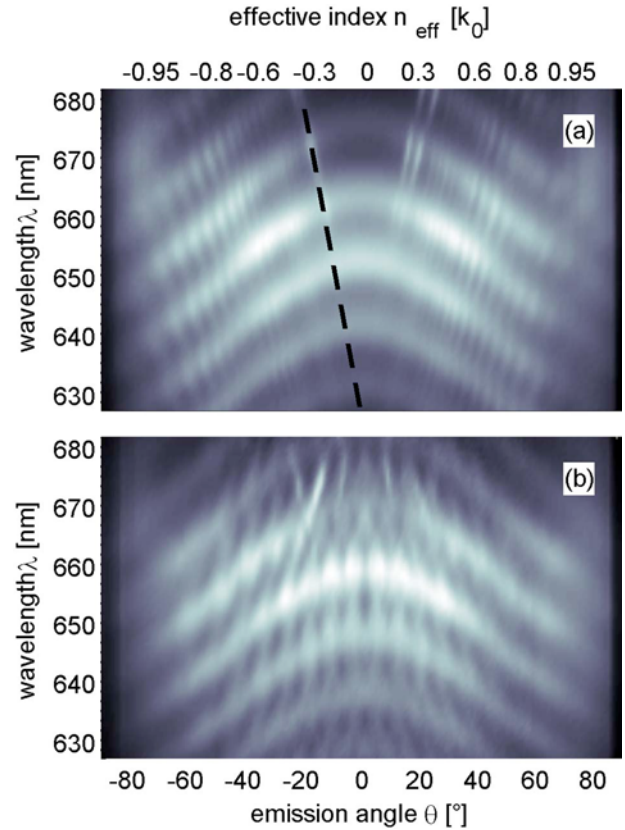


FIG. 3. (Color online) (a) Normalized spectral resolved farfields for hexagonal PhC-LEDs in the ΓM direction (a) $G=3.4 k_0$. The calculated type I mode with highest intensity has been inserted (dashed line). (b) $G=1.7 k_0$. Strong diffraction of type III modes at all wavelengths. NB The θ - λ representation used here is similar to the commonly used ω - k representation for guided modes.

affected by the distant PhC and so will only extract weakly. A second type (II) of modes with $n_{\text{PhC}} < n_{\text{eff}} < n_{\text{MQW}}$ are guided within the whole LED. These modes also interact only weakly with the PhC since they are evanescent within the PhC. A third range of modes (III) with $1 < n_{\text{eff}} < n_{\text{PhC}}$ interacts more strongly with the PhC. The simulation shows that this third type of modes is the most promising to extract due to its high coupling strength with the PhC, which explains the maximum extraction efficiency observed for $G/k_0 \approx n_{\text{eff}}=1.6$, as this effective index falls within the range of type III modes.

Spectrally resolved farfield patterns (Fig. 3) were collected with a scan step of 1° and 0.9° angular resolution. The farfields were normalized with the integrated emission spectrum and divided by a lambertian emission profile to visualize the PhC effect for all wavelengths and angles. In addition to the Fabry-Pérot resonances evidenced by the broad “boomerang”-shaped lines, the PhC-LED farfields have steep diffraction lines [Figs. 3(a) and 3(b)] that correspond to extracted guided modes. In the farfield pattern from a hexagonal PhC-LED with $G=3.4 k_0$ [Fig. 3(a)], two strong lines can be also observed near the top of the graph, around 670 nm. These lines disappear for wavelengths shorter than $\lambda_{\text{peak}}=658$ nm, indicating that these modes are reabsorbed in the active region much faster than they are extracted by the PhC. These lines should therefore correspond to type I modes and this is confirmed by the good agreement with the diffraction line (inserted dashed line) from the type I mode with highest

intensity calculated with a one-dimensional mode solver. Extracted type II and type III modes on the other hand, suffer less from reabsorption, since they have a lower overlap with the active region and the diffraction lines can be observed over the whole spectrum [Fig. 3(b)]. The slope of the diffraction lines shows that the extraction angle is almost independent of the wavelength within the emission spectrum, which highlights the fact that the diffraction strength is not sensitive to wavelength shifts that can be induced by heating or high current densities.

The highest PhC extraction enhancement at 10 mA compared to an unstructured reference is 47% for a 800 nm deep A7 lattice with $G=1.5 k_0$. Hexagonal and A7 PhCs do generally have very similar enhancement factors, as shown in Fig. 2(d). This was also observed in Ref. 9, suggesting that the total extraction efficiency is not enhanced by the A7 lattice despite its omnidirectional diffraction properties. The external quantum efficiency for this PhC-LED is 19% without encapsulation.

For comparison, the extraction efficiency for an unpatterned LED calculated with the formalism given in Ref. 10 is just $\eta_{\text{extr}}=3.5\%$. The measured $\eta_{\text{QE}}=\eta_{\text{int}}\eta_{\text{extr}}$ is 13%, however, where $\eta_{\text{int}}\leq 100\%$ is the internal quantum efficiency. This significant discrepancy between simulation and experiment can only be explained by photon recycling. In fact, simulations have shown that the light extraction efficiency can indeed be enhanced by a factor of this magnitude when η_{int} is close to 100%.¹¹ The mechanism for this almost four-fold enhancement is the reabsorption of preferentially guided modes in the active MQW region followed by re-emission into any mode. Hence, photon recycling redistributes the mode intensity such that more light is emitted into the light extraction cone. Type I modes are absorbed most strongly due to their high overlap with the MQW region but recycling also occurs for type II and type III modes.

Even though the extraction enhancement of 47% facilitated by the PhC is significant, much higher enhancements have been reported by other researchers, e.g., values $>100\%$ (Ref. 12) have already been achieved. These high values have been reported for AlGaInP LEDs with absorbing GaAs substrates and small emission windows, however, i.e., the high relative enhancement was obtained for devices with low absolute efficiency. Our results, in contrast, highlight the fact that significant enhancements can also be achieved for devices with high absolute efficiency.

Compared to surface roughening,^{13,14} our enhancement values are also lower. Surface roughening effectively scatters incident light randomly into all directions. Hence, a fraction

of the light is extracted regardless of the effective index of the incident light. In contrast, the PhC extracts a limited mode range with high efficiency but the remaining modes are not extracted at all [Fig. 2(a)]. In principle, this enables the extraction of light into a limited extraction cone, i.e., the creation of a more directional beam. Therefore, a much thinner device with a tailored mode distribution⁴ is expected to show higher PhC enhancements.

In summary, we have fabricated and characterized Al-GaN thin-film LEDs with 200 and 800 nm deep hexagonal and Archimedean A7 PhCs with different lattice constants. Spectral farfield measurements show the multimode extraction and that the extraction angle of a single mode is almost constant over the spectral emission width. The highest extraction enhancement of 47% is obtained for extraction of high-order type III modes, which is in agreement with simulations based on coupled mode theory. The main achievement reported here is the demonstration of high PhC-based extraction enhancement combined with a high absolute external quantum efficiency.

¹S. Fan, P. R. Villeneuve, J. D. Joannopoulos, and E. F. Schubert, *Phys. Rev. Lett.* **78**, 3294 (1997).

²A. A. Erchak, D. J. Ripin, S. Fan, P. Rakich, J. D. Joannopoulos, E. P. Ippen, G. S. Petrich, and L. A. Kolodziejski, *Appl. Phys. Lett.* **78**, 563 (2001).

³M. Rattier, H. Benisty, E. Schwoob, C. Weisbuch, T. F. Krauss, C. J. M. Smith, R. Houdre, and U. Oesterle, *Appl. Phys. Lett.* **83**, 1283 (2003).

⁴A. David, T. Fujii, R. Sharma, K. McGroddy, S. Nakamura, S. P. DenBaars, E. L. Hu, C. Weisbuch, and H. Benisty, *Appl. Phys. Lett.* **88**, 061124 (2006).

⁵J. J. Wierer, M. R. Krames, J. E. Epler, N. F. Gardner, M. G. Craford, J. R. Wendt, J. A. Simmons, and M. M. Sigalas, *Appl. Phys. Lett.* **84**, 3885 (2004).

⁶D.-H. Kim, C.-O. Cho, Y.-G. Roh, H. Jeon, Y. S. Park, J. Cho, J. S. Im, C. Sone, Y. Park, W. J. Choi, and Q.-H. Park, *Appl. Phys. Lett.* **87**, 203508-1 (2005).

⁷C. Wiesmann, K. Bergenek, N. Linder, and U. T. Schwarz (unpublished).

⁸K. Streubel, N. Linder, R. Wirth, and A. Jaeger, *IEEE J. Sel. Top. Quantum Electron.* **8**, 321 (2002).

⁹A. David, T. Fujii, E. Matioli, R. Sharma, S. Nakamura, S. P. DenBaars, C. Weisbuch, and H. Benisty, *Appl. Phys. Lett.* **88**, 073510 (2006).

¹⁰J. A. E. Wasey and W. L. Barnes, *J. Mod. Opt.* **47**, 725 (2000).

¹¹P. Altieri, A. Jäger, R. Windisch, N. Linder, P. Stauss, R. Oberschmid, and K. Streubel, *J. Appl. Phys.* **98**, 1 (2005).

¹²T. Kim, A. J. Danner, P. Leisher, K. D. Choquette, R. Wirth, and K. Streubel, *IEEE Photonics Technol. Lett.* **18**, 1876 (2006).

¹³R. Wirth, S. Illek, C. Karnutsch, I. Pietzonka, A. Plössl, P. Stauss, W. Stein, W. Wegleiter, R. Windisch, H. Zull, and K. Streubel, *Proc. SPIE* **4996**, 1 (2003).

¹⁴R. Windisch, C. Rooman, S. Meinschmidt, P. Kiesel, D. Zipperer, G. H. Döhler, B. Dutta, M. Kuijk, G. Borghs, and P. Heremans, *Appl. Phys. Lett.* **79**, 2315 (2001).